ELSEVIER

Chemical Engineering Journal 77 (2000) 127–135

Chemical Engineering Journal

www.elsevier.com/locate/cej

First demonstration of optical fluorescence auto-projection tomography

Francis Hindle, Hugh McCann *, Krikor B. Ozanyan

Department of Electrical Engineering and Electronics, UMIST, PO Box 88, Sackville Street, Manchester, M60 1QD, UK

Abstract

A novel concept is introduced for application to chemical species tomography. The technique is based on fluorescence, using collimated sources and detectors. It does not require a complex inversion step to calculate the distribution of the desired parameter. Suitable gaseous fuels, dopants, and sources are assessed for potential use in a fuel imaging system within an internal combustion engine. The technique has difficulty in meeting the temporal requirements in such a gas-phase application. However, first data are presented from liquid-phase experiments that demonstrate the technique in operation.

Keywords: Fluorescence; Tomography; Fuel; Visualisation

1. Introduction

A wide range of tomographic modalities have been developed over several decades, encompassing the classes of hard-field, soft-field and emission techniques [1]. All of these different classes have their various strengths and weaknesses in a range of applications. In particular, they all require an inversion calculation to reconstruct the distribution of the parameter of interest [2].

One particularly interesting option, which fits none of the above classes, is fluorescence tomography: the stimulation process has a 'hard-field' nature in that the only material affecting the traversal of the stimulation beam through the subject is that which is in the geometrical path, whilst the isotropically emitted fluorescence clearly has an 'emission' nature [3]. The early development of such a system is reported here, with the first demonstration data.

As discussed elsewhere [4], spatial variation of air–fuel ratio in an internal combustion engine is of great commercial and environmental interest. Optical tomographic determination of this parameter has several potential advantages over other techniques, such as Planar Laser-Induced Fluorescence (PLIF) [5,6], notably that optical access is required in one plane only. Hence, the fuel–air mixture is the target subject for the present system development, and its specific requirements are discussed in Section 2. Subsequent experimental data (Sections 3–6) show that the temporal resolution of this application is particularly demanding, with present stimulation sources. In Section 2.3, liquid-phase data are presented, in order to illustrate the principle of the technique in operation.

2. Concept

2.1. General

In the case of X-ray fluorescence, Cesareo and Mascarenhas [7] have pointed out that collimation of both the stimulation beam and the detector acceptance results in an unambiguous determination of the spatial region (hereinafter termed 'space-point' or 'voxel') from which the signal was emitted. In their case, where they examined a relatively dense host, significant attenuation of both the stimulation beam and the fluorescence signals required additional complexity to calculate the distribution of the measured parameter. The need to account for the subject's attenuation can be removed by the selection of a species with lower absorption, for example gaseous fuels diluted in air. The resulting measurements can be used to determine the parameter of interest at a number of space-points followed by a simple calculation to obtain the distribution or 'image' required. We call this property 'Auto-Projection', since it is pre-determined by the geometry of the system. Each measurement is automatically projected onto real space so an image can be produced without performing a difficult inversion step, as is used in conventional tomography.

Hence, the term 'Auto-Projection Tomography' (APT) refers to the use of collimated sources and detectors to determine unambiguously a parameter of interest at a number of geometrically defined space-points within a larger

* Corresponding author.
E-mail address: h.mccann@umist.ac.uk (H. McCann).

1385-8947/00/$ – see front matter
PII: S1385-8947(99)00143-6

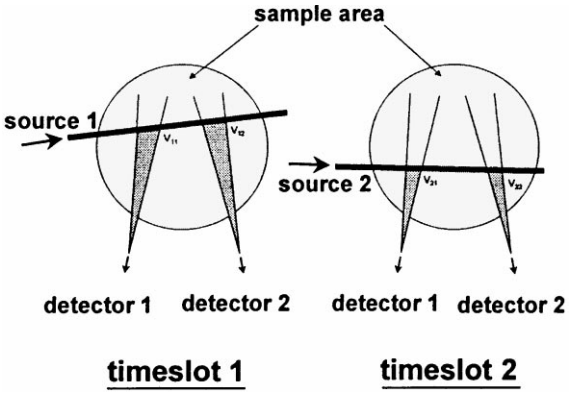

Fig. 1. 2×2 Auto-projection system.

subject of limited absorption. In the optical domain this can be achieved by exploiting the fluorescence of the species of interest to measure its concentration. The spatial intersection of a particular source beam and the acceptance aperture of a particular detector define a unique space-point, from which any signal contribution must have originated, if no other source was active during the measurement. Thus, APT allows 'true' 3-dimensional mapping if the excitation beams do not lie in a single plane. In such a case the 3-dimensional image results from direct measurements and not by stacking of separate 2-dimensional 'slices'. A system with N independently controllable sources and M detectors will provide $N \times M$ space-points. In the remainder of this paper, all stimulation beams and detector apertures lie in a single plane.

An Optical Fluorescence Auto-Projection Tomography (OFAPT) system with two sources and two detectors requires two measurement periods to resolve four space-points (see Fig. 1). During the first period, Source 1 is active while both detectors are sampled; in the second period Source 2 is active while both detectors are sampled.

Even moderate values of N and M can result in large numbers of space-points. Provided there are sufficient distributed space-points, then interpolation between the space-points will allow the parameter calculation of the entire subject.

The parameter reconstruction step [1] of more conventional tomographic modalities is more complex since each detector is sensitive to path-integrated contributions across the subject for hard-field modalities, or contributions from the whole of the subject (in principle) for soft-field modalities.

Critical requirements for an OFAPT system are that the fluorescence properties of the subject are well known, and that the stimulation sources have to be operated sequentially during the acquisition of data for a single image. The fundamental issue in developing this technique is the trade-off between the need for spatial and temporal resolution on the one hand, and the requirement to have a suitably strong and quantifiable fluorescence signal on the other. This is developed further in Section 5.

2.2. Automotive R&D

The original development of the OFAPT system discussed here has been focused on a fuel imaging system for internal combustion engines. PLIF is a widely used technique to visualise fuel within an engine: a laser is formed into a sheet, passed through the engine, and fluorescence is observed in an orthogonal direction, typically with a CCD camera [6,8].

In the Stokes mechanism [9], incident photons are absorbed by molecules, resulting in emission of photons of a longer wavelength (red shifted) than the absorbed photons. This fluorescent emission is used to measure the subject's concentration via the relationship [10]:

$$I_F = 2.303 \times I_O K \phi_F \varepsilon c x, \quad \varepsilon c x < 0.05 \tag{1}$$

where I_O and I_F ($\mathrm{mW\,mm^{-2}}$), are intensities of the incident and emitted light, respectively; the fluorescence properties of the species are given by extinction coefficient, ε ($\mathrm{l\,mol^{-1}\,cm^{-1}}$) and quantum efficiency, ϕ_F; c is the concentration of the subject ($\mathrm{mol\,l^{-1}}$) and x is the path length of the stimulation beam through the space-point (cm); K is a combined geometrical and optical factor, which represents the collection efficiency for the emitted photons.

The Stokes mechanism has been exploited [11,12] to measure species such as OH, O_2, and NO in flames, by the laser excitation of particular electronic transitions, and wavelength-resolved detection.

In PLIF engine studies, the fluorescent species is often the fuel or a dopant contained in the fuel [6]. The large number of pixels of CCD cameras and the short, high power laser pulse ensure adequate spatial and temporal resolutions of the images captured. However, the orthogonal optical access required is intrusive in the sense that severe modifications to the engine are necessary: large glass inserts are placed between the cylinder head and the engine block allowing the laser sheet to pass through the top of the combustion chamber; an elongated piston with a window in the centre is used with a mirror to provide the CCD with a 'through-piston' view of the laser sheet. The result is a complex opto-mechanical solution which is difficult to implement even on research engines. The image framing rate of PLIF systems is severely restricted by the low repetition rates (0.1–100 Hz) [5] of the lasers. Nevertheless PLIF systems do resolve real space-points.

The degree of optical access required for an OFAPT system can be low compared with PLIF, as the excitation and detection beams can lie in the same cross-section plane of the engine cylinder. Using optical fibres [13] to deliver the light to and from the combustion chamber can decrease intrusion further. A series of sequentially operated light sources at a suitable wavelength will allow an OFAPT system to operate at an increased framing rate. The ideal is to capture consecutive frames, each with a temporal resolution of 1° crank angle (CA) rotation, for an engine running at say, 1000 rpm. In such a case, the time available for the operation of each

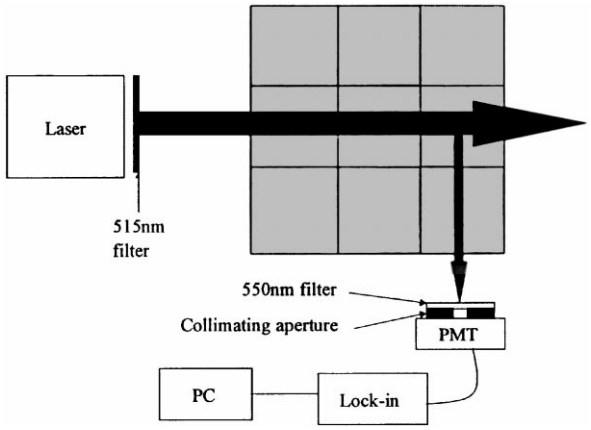

Fig. 2. Liquid-phase OFAPT apparatus.

of the N sources and the measurement of each space-point is $(167/N)\,\mu s$.

2.3. Liquid-phase OFAPT experiment

The OFAPT technique was demonstrated by making space-point measurements within a liquid subject. Nine cells were assembled into a 3×3 grid. Each cell was filled with water, and a small quantity of rhodamine 6G dye was added to some cells to provide an inhomogeneous distribution to be imaged. The maximum concentration of dye was limited to yield an absorption of 3.5% per cell. The measurement of each space-point was made by placing the laser and a Hamamatsu H5783-03 Photo Multiplier Tube (PMT) module at 90° to each other and aligning them to the centre of the particular cell under examination (see Fig. 2). In this case a total of nine measurements are required to characterise the distribution.

The multiple wavelength output of a Laser Physics Reliant 150M Argon ion laser was filtered by an interference filter ($\lambda_{centre} = 515$ nm; Full Wave Half Maximum (FWHM) = 10 nm) delivering 0.6 mW at 514 nm, a suitable stimulation source for rhodamine 6G. The detection filter was made from OG550 glass (550 nm long pass).

The system was calibrated by placing an object in each cell and measuring the system response for each space-point. A matrix containing these space-point system response factors is then used to calculate the normalised space-point dye concentrations for data measured with an unknown dye distribution.

Figs. 3 and 4 show the real and measured dye concentration distributions. The errors observed when comparing the real and measured distributions are dominated by the scattering of the laser by the cell walls and the poor collimation of the PMT detectors. The observed signal strengths for a normalised dye concentration of 1 was ≈4 nW which is 2 orders of magnitude greater than obtained during the gas-phase experiments (see Section 6.2).

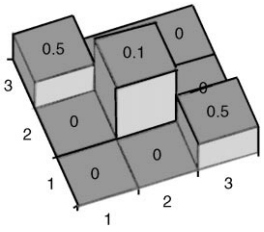

Fig. 3. Real distribution of dye concentration.

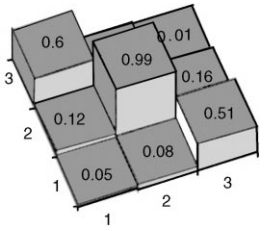

Fig. 4. Measured distribution of dye concentration.

2.4. Other fields of interest

Fluorescence imaging has been widely used in a range of fields, from biomolecular sciences to chemical engineering. Typically, these studies also require multi-plane optical access, although their temporal requirements are much less severe than the internal combustion engine case. Furthermore, in cases where liquid-phase systems are studied [14,15], the signal yield is much larger as seen from Eq. (1).

3. Fluorescence spectra

3.1. General

The fluorescence of several chemical systems has been studied, ranging from 3-pentanone diluted in iso-octane, to a range of commercial gasolines. In the selection [16] of a fluorescing species the following properties must be considered:

- $\varepsilon(\lambda)$, absorption of the incident beam.
- $\phi_F(\lambda)$, conversion efficiency of absorbed photons to fluorescence photons.
- Magnitude of the Stokes red shift.
- Emission dependence upon temperature and pressure.
- Fluorescence quenching by oxygen.
- Re-absorption.

The extinction coefficient and quantum efficiency are functions of excitation wavelength, and their product effectively determines the realistic range within which the stimulation system must operate. The red shift exhibited by a species must be sufficient to allow filtration of the emitted and/or stimulation light, thereby minimising any elastically scattered stimulation light seen by the detection system. Pressure, temperature, oxygen quenching and re-absorption

may significantly influence the detected fluorescence intensity. Re-absorption describes a mechanism whereby photons fluoresced from a molecule are absorbed by another molecule present in the subject. The majority of information which may be gathered from an engine study will be at the maximum compression of the cylinder (≈1 MPa for a spark ignition engine) and high temperature (≈400 K).

3.2. Dopants

If the fuel used is composed of a non-fluorescing base and a fluorescing dopant, then the dopant must be readily soluble in the base and have a similar boiling point. Such a fuel will allow the desired absorption to be achieved by controlling the dopant concentration.

3-Pentanone ($C_5H_{10}O$) is often used in PLIF studies to dope iso-octane (C_8H_{18}). Research grade or High Performance Liquid Chromatography (HPLC) grade iso-octane does not fluoresce [6,8]. Hansen [17] has determined the extinction coefficient, quantum efficiency and emission of 3-pentanone. The variation of these properties with temperature, pressure, and oxygen quenching, have been studied [6,8] and found to be favourable for combustion studies in which iso-octane is the base fuel. (This is a commonly used fuel in engine and combustion research and development.) It is worth noting that the peak absorption of 3-pentanone occurs at 285 nm (FWHM = 45 nm) and peak emission at 430 nm (FWHM = 120 nm), displaying sufficient Stokes shift to be useful. Since the quantum efficiency is effectively independent of wavelength, the excitation spectra will have the same shape as the absorption spectra. This is provided for comparison with the excitation spectra of gasoline in Fig. 5. Excitation spectra represent the ability of a species to absorb incident photons and relax the excess energy by fluorescing photons, as a function of excitation wavelength. They may be measured using a fluorimeter with a fixed emission wavelength and scanning a range of excitation wavelengths.

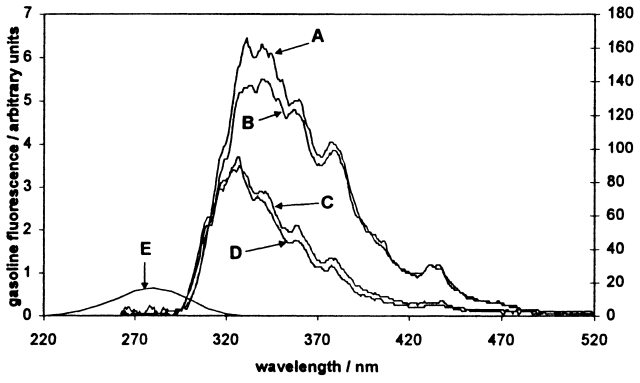

Fig. 5. Excitation spectra of gasoline compared with the absorption of 3-pentanone [17]. 2nd *y*-axis 3-pentanone molar extinction coefficient/l mol^{-1} cm^{-1}. (A) Super with no additives, (B) Super with 2 × additives, (C) Normal with 2 × additives, (D) Normal with no additives, (E) 3-Pentanone (2nd *y*-axis).

Table 1
Properties of typical aromatic [18] species found in gasoline, along with 3-pentanone [17] data for comparison

Aromatics	Boiling point °C	Quantum efficiency
Benzene	80	0.07
Toluene	111	0.17
Ethyl benzene	136	0.18
Meta-xylene	138	0.17
Para-xylene	138	0.40
Ortho-xylene	144	0.19
1,3,5-Trimethylbenzene	170	0.12
1,2,4-Trimethylbenzene	148	0.41
3-Pentanone	102	0.0025

3.3. Gasolines

The excitation spectra for a number of gasolines were determined, see Fig. 5. The gasolines were diluted in 10 parts of HPLC grade iso-octane. A typical gasoline contains approximately 35% aromatic hydrocarbons. These components can be studied and the fluorescence properties of each assessed [18].

The data in Table 1 show that gasoline contains species with quantum efficiency 2 orders of magnitude larger than that of 3-pentanone. The higher fluorescence signal from 'Super' grade gasoline, compared with 'Normal' in Fig. 5, is due to the higher aromatic content. The red shift observed in these species is significantly smaller than for 3-pentanone. The fluorescence properties of a full gasoline mixture in a combustion environment have been found to be less favourable than for 3-pentanone [16], i.e. in terms of oxygen quenching, re-absorption, pressure and temperature effects. A severe decrease in emission was experienced at the elevated pressures in a running engine.

4. Assessment of the technological options

4.1. Sources

The nature of the optical sources for stimulation of fluorescence is the most critical aspect of OFAPT system design. The source requirements for an OFAPT system are:

- Multiple sources
- Sequential operation
- Wavelength in a suitable range
- Adequate power
- Fibre coupling for engine application

The requirement for sequential operation can be achieved by a number of discrete sources centrally controlled, one source scanned over multiple light channels, or one source divided equally into a number of light channels with intensity modulation of each channel. For the gas-phase engine application, an OFAPT system with 10 sources must be able to operate with a maximum pulse duration of 17 μs (see Section 2.2).

The sequential operation and UV wavelength required for the stimulation of 3-pentanone (285 ± 25 nm) present considerable difficulty in identifying a suitable OFAPT source. In the gasoline case, fluorescent species are normally present (although generally less well understood than 3-pentanone), which yield strong signals upon stimulation over a wider range of wavelengths. Sources in the range of 300–500 nm may be considered for the stimulation of gasoline, as seen in Fig. 5.

For OFAPT, the critical parameter for any source is the total energy delivered, $E_{P,}$ for each fluorescence sampling period. We use this parameter below, for a sampling period of 17 μs, to compare sources and assess the power requirements for an internal combustion engine OFAPT fuel imaging system (see Section 6.2). However, it is important to consider the possibility of saturating the fluorescent emission, or the detector during, the stimulation period. E_P is provided only for the ease of comparison between different sources.

4.1.1. Discharge lamps

Deuterium lamps [19] provide broadband emission from 200 to 400 nm. A complex drive circuit is required for sequential operation of multiple lamps. Optical filtering would be necessary to remove the visible component of the lamps' output.

Higher power Xenon discharge sources could be implemented as a single source scanned over a number of fibres or coupled to multiple fibres. Scanning could be achieved using a rotating mirror. Alternatively a multi-faceted opto-mechanical chopper rotating at approximately 90 Hz could modulate multiple fibres coupled to one lamp. The scanning and chopping solutions would both result in a complex opto-mechanical construction along with a significant insertion loss. Neglecting insertion losses, we calculate that these sources yield $E_P = 340$ nJ.

4.1.2. Semiconductor sources

Semiconductor sources offer a more convenient method of providing the sequential source operation required in an OFAPT system. Unfortunately there are no semiconductor devices available at present capable of providing UV radiation for the stimulation of 3-pentanone.

Blue laser diodes [20] have been reported by Nichia, yielding 50 mW at 410 nm. These could be considered for use in a final system but the schedule for commercial availability of the diodes is not clear. These devices promise $E_P = 850$ nJ.

LEDs are low cost, low power discrete sources, available in the blue region with nominal wavelengths of 430 and 470 nm, FWHM of 40 nm, and approximately 2 mW power output. Although difficult to couple to fibre efficiently, they are convenient to drive sequentially. Pulsed operation with a low duty cycle can allow an increase in the available peak power by a factor of 10 or so. We calculate $E_P = 340$ nJ for these sources.

4.1.3. Pulsed lasers

The Nd:YAG and excimer lasers [5] used in conventional PLIF studies produce very intense (10–100 mJ) short (10 ns) pulsed outputs at a wavelength suitable for 3-pentanone excitation. However they operate at a typical repetition rate of 1 Hz with a maximum of 100 Hz, which is 2 to 3 orders of magnitude slower than required for the 1° CA frame rate target. Typically, $E_P = 10$ mJ in this case. For comparison with an OFAPT system comprising, say 20 sources, the equivalent E_P of PLIF is 500 μJ, since the light is delivered to the whole cross-section rather than to individual space-points.

A Ce:LiCAFv [21] laser pumped with a copper vapour laser can yield up to 450 mW average power output at a wavelength of 288.5 nm with a repetition rate of 7 kHz and a 8 ns pulse length, yielding $E_P = 64$ μJ. Whilst the requirement of a copper vapour laser and custom built non-linear optical apparatus is significant, this option has promise if in-fibre multiplexing can be achieved.

Frequency-quadrupled Nd:YAG lasers are capable of producing high average powers with repetition rates above 5 kHz [22]. Operating at 1 kHz an average power of 2.8 W was obtained at 266 nm i.e. $E_P = 2.8$ mJ. As this laser is not presently available as a commercial product, a custom non-linear optical setup must be constructed. Nevertheless, the E_P value for this source is very attractive.

4.1.4. Continuous wave lasers

Gas lasers at suitable wavelengths are 325, 442 nm (HeCd) and 300, 457, 488 nm (Argon ion). These lasers can deliver approximate powers of 1 mW to 1 W, yielding $E_P = 17$ nJ to 17 μJ. Electro-optic or acousto-optic deflectors may be used to scan the laser over a number of fibres. Such deflectors are commercially available along with the necessary high-frequency drive electronics. Electro-optic deflectors capable of producing deflections in the region of 1 mrad/kV have been demonstrated [23] and should be suitable for use down to 300 nm. Acousto-optic deflectors are available for use down to 360 nm.

Blue frequency-doubled lasers producing 15 mW at 430 nm ($E_P = 255$ nJ) are commercially available [24] and have very similar characteristics to the blue laser diode presently under development by Nichia [20]. This laser may be modulated directly.

4.2. Optics

4.2.1. Launch

The characteristics of the launch optics will depend greatly on the source and modulation technique selected. The ideal performance of the launch optics would be to provide a collimated beam with a known path across the subject. The total fluorescence signal within the field of view of the detection system is independent of the source cross-section area. Therefore a badly collimated beam can be tolerated, within the limits of the system spatial resolution and the detector field of view.

4.2.2. Receive

The collection optics are required to gather fluorescence from defined space-points distributed over the entire subject. The optics for each detector must therefore have a limited field of view. The degree of restriction will define the spatial resolution and the magnitude of any measurements made. An additional problem to consider is the dependence of the signal magnitude upon the space-point-to-detector distance. This can be expressed within the factor K (Eq. (1)), in terms of the proportion of the isotropically emitted fluorescence collected. If a conical collection scheme is employed, the space-point-to-detector distance dependence is reduced. However, the space-point size and hence spatial resolution of the system then become functions of the space-point-to-detector distance.

4.3. Detectors

The minimum resolvable power levels of the detectors will directly influence the total stimulation power required to perform the species concentration measurements with the desired resolution and signal to noise ratio. Each detector and associated amplifier must have a sufficient bandwidth to allow sampling during the active period of each source, with appropriate noise suppression. Good temporal resolution with gas-phase subjects puts a considerable premium on low-noise detection technology.

5. Calculation of fluorescence intensity

The factors influencing the intensity of observed fluorescence have been incorporated into a calculation scheme which, for a given optical configuration, yields the ratio of fluorescence intensity to excitation intensity (I_F/I_O) see Eq. (1). For the purposes of illustration, the total path absorption of a stoichiometric homogenous mixture was defined as 5%, which is a reasonable value for various cases. The path was divided into r space-points ($r = 8$, 16, or 32) and the absorption of each space-point determined for the above conditions using the following relationship between path and space-point transmissions.

$$T_{\text{Space-point}} = (T_{\text{path}})^{1/r} \quad (2)$$

Fig. 6 shows I_F/I_O for a measurement of a space-point at the centre of an 80 mm diameter combustion chamber, using a 1.5 mm diameter collection lens and iso-octane doped with 3-pentanone ($\Phi_F = 0.0025$). The concentration of 3-pentanone is fixed by the space-point absorption obtained from Eq. (2) above.

With knowledge of I_F/I_O, and the minimum resolvable power of the detection system, the stimulation power required to perform the fuel concentration measurements with the desired accuracy and resolution can then be determined.

To view the above in the context of the present application, it should be noted that a stoichiometric mixture at 1 MPa and 400 K will give a total path absorption of 10% ($\lambda = 285$ nm) with a 19% dopant to fuel ratio; this is typical [6]. Note also that the fluorescence yield of any other species in the above calculation will scale simply in the ratio of the quantum efficiencies, neglecting any quenching effects.

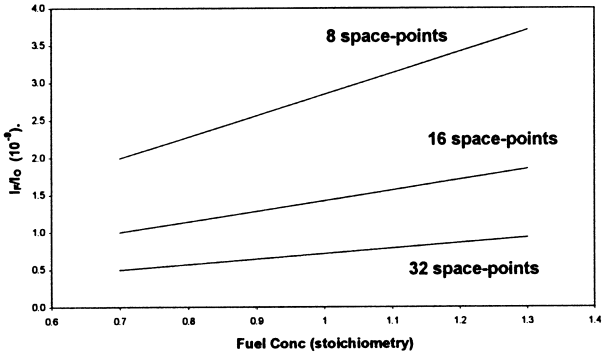

Fig. 6. I_F/I_O per space-point vs. Fuel Concenteration, with the path divided into various numbers of space-points (total path absorption 5%).

The following assumptions have been made:

- No light is scattered during traversal to or from the fluorescing space-point.
- The stimulation and detection of a space point are orthogonal to one another.
- The fluorescence source is a point in the centre of the space-point.
- Fluorescence saturation is not reached.
- The extinction coefficient for 3-pentanone is dominant.

For the gas-phase case, it should be noted that the I_F/I_O values in Fig. 6 are of the order of 10^{-9}, which indicates that a very intense source ($\approx$1 W) would be necessary in order to apply this technique for 3-pentanone/iso-octane in the present case.

6. Experimental work

6.1. Single point liquid-phase

As a preliminary step to gas-phase experiments, a simple system was established to measure the fluorescence of a liquid-phase sample contained within a cuvette (Fig. 7).

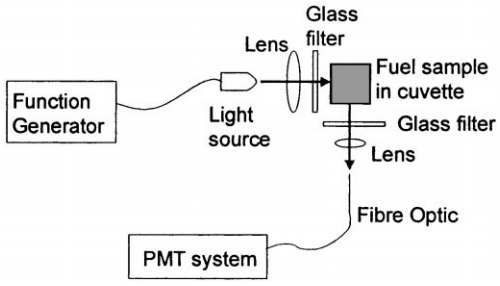

Fig. 7. Liquid-phase fluorescence system.

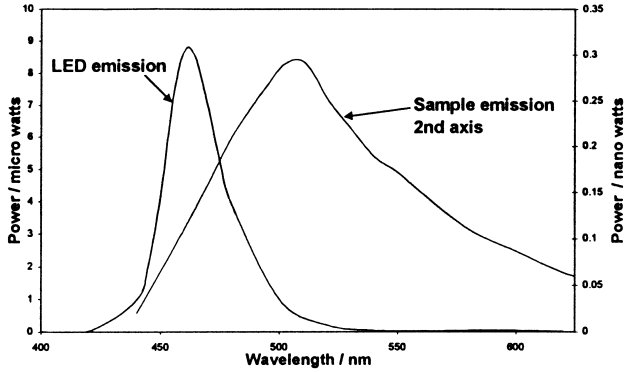

Fig. 8. Spectral analysis of blue LED and gasoline fluorescence.

The system was operated with either a bright blue LED or a Deuterium lamp. Effects of scattered light were minimised by inserting appropriate glass filters, and using perpendicular source and detection light paths. Fluoresced light could be delivered to the photomultiplier tube by either a 200 or 500 μm diameter fibre optic.

6.2. Gasoline

The signal obtained from a gasoline sample, diluted in iso-octane and stimulated by a blue LED, was directly confirmed to be fluorescence by performing a spectral analysis of both the source and the emitted light using a computer-controlled scanning monochromator. The spectra in Fig. 8 show the red shifted fluorescence signal compared with the LED spectrum.

As expected, increased emissions were observed at higher gasoline concentrations. The LED peak emission wavelength of 460 nm corresponds to a weak absorption region on the gasoline excitation spectrum, as shown in Fig. 5. A shorter wavelength source would yield a stronger fluorescence signal per unit of stimulation power. Blue LEDs are capable of producing fluorescence from gasoline, but are unlikely to provide sufficient fibre-coupled power for an OFAPT system where the gaseous sample concentration is 3 orders of magnitude lower than for a liquid, and the measurement space-point is distant from the collection lens. Alternatively, more intense blue sources, as discussed in Section 4.1, may provide a desirable solution.

6.3. 3-Pentanone

A deuterium lamp provided UV radiation at 285 ± 25 nm to stimulate 3-pentanone. The lamp output was filtered using a glass UG5 filter to remove wavelengths longer than 410 nm. A suitable dopant concentration was determined by performing a number of transmission tests using a Cathodeon J18 deuterium lamp, a Cathodeon C710 power supply, a Bentham M300EA monochromator and a Newport 1830-C power meter. Weak fluorescence was observed with a PMT. Lamps with smaller apertures are available and are four times brighter. Intensities can be further increased by pulsing the lamps at a low duty cycle, allowing an additional increase up to seven times in lamp intensity. Although a small-aperture, pulsed, fibre-coupled deuterium lamp will give a reasonable fluorescence signal with 3-pentanone, the intensity is too low for implementation into a real system where the measurement space-point may be located in the centre of the combustion chamber.

Table 2
Liquid fluorescence results

Light Light	Subject	Fibre diameter (μm)	Signal captured (photon/μs)
LED	Gasoline	500	1027
LED	Gasoline	200	86
D2	3-Pentanone	500	6
D2	Gasoline	500	216

All the liquid-phase experiments were conducted with an identical optical arrangement and detection system (Fig. 7). The results from the liquid-phase experiments (Table 2) show that the intensity of the 3-pentanone fluorescence was much weaker than that of gasoline, as expected. The geometrical coupling in the liquid-phase experimental system is significantly higher than would be expected in a real system where the space-point-to-detector distance may be the radius of a combustion chamber (≈40 mm). The space-point-to-detector distance in the liquid-phase experiment was approximately 8 mm, implying a signal reduction factor of 25 if the distance is increased to 40 mm.

6.4. Single point gas-phase

A single point gas-phase gasoline experiment was performed using a pressure vessel fitted with windows (see Fig. 9). The vessel was heated to 200°C to ensure complete vapourisation of the fuel. The multiple wavelength output of a Laser Physics Reliant 150 M Argon ion laser was filtered by an interference filter ($\lambda_{centre} = 458$ nm, FWHM of 10 nm) delivering laser light at 457 nm to the subject. This wavelength although not ideal for absorption by gasoline (see

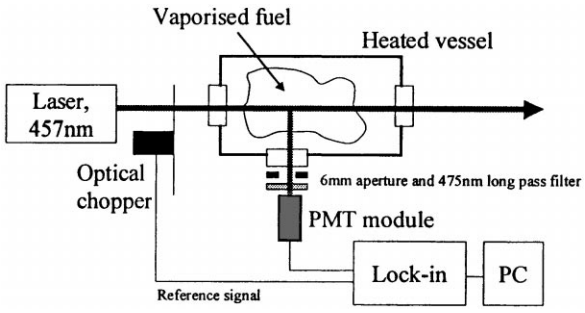

Fig. 9. Experimental apparatus for single point gas-phase measurements.

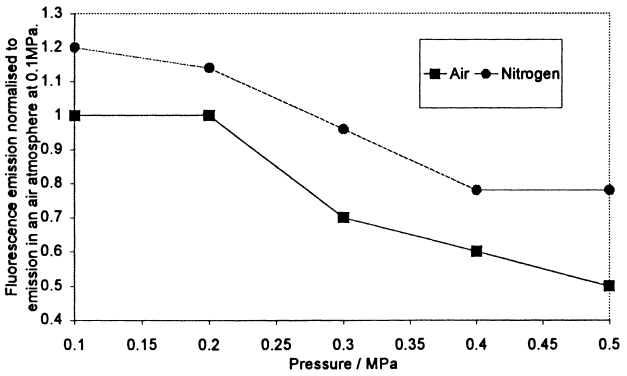

Fig. 10. Emission from gasoline at elevated pressures in air and nitrogen environments.

Fig. 5) will provide sufficient information to quantify gasoline fluorescence over a range of stimulation wavelengths.

Measurements were taken in both air and nitrogen atmospheres at pressures from 0.1 to 1 MPa (see Fig. 10). Note that a fixed volume of fuel was used, effectively weakening the mixture at increased pressures, i.e. the fluorophore concentration was fixed while the pressure was increased. At pressures greater than 0.5 MPa the fluorescent signal was not large enough to distinguish from the scattered signal. Fluorescence signals were compared with 475 (GG475) and 495 nm (GG495) long pass filters to confirm the emission was located in the 460–480 nm region.

The data in Table 3 were taken with 0.82 mW of stimulation power reaching a homogeneous subject with a fuel concentration of $6 \times$ stoichiometry and at a total pressure of 0.1 MPa. The detector was positioned 60 mm from the space-point with a useable area of 28 mm^2. The stimulation path length viewed by the detector was 4 cm (see x in Eq. (1)).

Ignoring any additional quenching resulting from increases in pressure these results indicate that to measure fuel concentration at a space-point 40 mm from a 2 mm diameter detection lens with 5 mm spatial resolution and $0.1 \times$ stoichiometry fuel concentration resolution, a minimum E_P of 165 nJ would be required at this wavelength. However the pressure effects must not be overlooked. The fluorescent emissions from a fixed quantity of fuel in a vessel at various pressures were measured (see Fig. 10). Each data point is a mean value of multiple experiments, the standard deviations of the data being 12% of the mean signal or smaller.

Table 3
Gasoline experiment: measured power levels

	pW
Scatter prior to fuel injection	4.0
Peak emission	21.6
Emission after 70 s	18.7

7. Discussion and conclusions

A tomographic system based on the OFAPT concept has been shown to resolve chemically specific information for real space-points and determine the distribution of the measured parameter using a simple calculation, viz. P multiplications for P pixels. The critical factors governing the successful operation of such a system are that the fluorescent properties of all the chemical species within the subject are well known and that sufficient stimulation can be sequentially delivered to each space-point.

Desirable properties for the fluorescing species are high quantum efficiency, suitable concentration levels to control absorption, sufficient Stokes shift, low dependence on other parameters and low re-absorption. The stimulation beam is exponentially attenuated by the subject, therefore the conflicting requirements of fluorescence stimulation and beam intensity uniformity across the subject must be met. If absorption or re-absorption effects are significant, additional complexity will be required to retrieve the desired information. In this case the advantages of making space-point measurements will have been diminished, as the received signal will not only be dependent on the value of the measured parameter at the space-point, but also the path integrated concentration of the absorbing and re-absorbing species along the two paths: from the source to the space-point and from the space-point to the detector.

The E_P value (Section 6.2), required for the combustion engine system does not include the losses associated with the use of fibre coupled launch and detection schemes which are convenient for an engine application. The gasoline emission discussed in Section 6.2 was found to be too weak in the case where the detector acceptance is determined by coupling into a 500 μm fibre. Therefore higher power and/or shorter wavelength sources are needed if the technique is to be applied to a fibre coupled combustion chamber imaging application. The optimum stimulation wavelength for gasoline is at its peak absorption of 330 nm (see Fig. 5). At present, ideal light sources meeting the above requirements do not exist for OFAPT combustion chamber gaseous fuel imaging. Deuterium lamps are not powerful enough for implementation into an OFAPT system for this application. Existing blue laser sources are not optimally suited to the absorption spectrum of gasoline. Blue semiconductor lasers appear promising in the medium term. In the longer term, pulsed lasers may provide a possible solution. There are many advantages in the use of a 3-pentanone dopant. However, its low quantum efficiency prevents its use with low intensity sources of light. The fluorescence of gasoline is less quantifiable than that of 3-pentanone. Gasoline fluorescence will not only vary from one batch to another but is likely to suffer from quenching and re-absorption especially at high pressure.

OFAPT does appear feasible with presently available light sources for applications with less demanding imaging rate requirements or stronger yielding subjects.

Acknowledgements

We thank EPSRC for supporting this work via a studentship for FH, and are grateful to our UMIST colleagues Stephen Carey for helpful discussions, and Eric Clough for assistance with the gas-phase cell.

References

[1] M.S Beck, R.A. Williams, Process Tomography: Principles, Techniques and Applications, Butterworth-Heinemann Ltd, Oxford, 1995.
[2] Avinash C. Kak, M. Slaney, Principles of Computerized Tomographic Imaging, IEEE Press, New York, 1988.
[3] G. Guilbault, Fluorescence, Theory, Instrumentation, and Practice, Arnold, London, 1967, pp. 1–3.
[4] S. Carey, H. McCann, D. Winterbone, E. Clough, Near Infra-Red Absorption Tomography for Measurement of Chemical Species Distribution, in: Proc. 1st World Congress Industrial Process Tomography, Buxton, UK, 1999.
[5] E. Winklhofer, H. Fuchs, Laser induced fluorescence and flame photography tools in gasoline engine combustion analysis, Optics Lasers Eng. 25 (1995) 379.
[6] M. Berckmüller, N. Tait, D. Greenhalgh, The time history formation process in a lean burn stratified-charge engine, SAE 961929 (1996) 77–98.
[7] R. Cesaro, C. Mascarenhas, A new tomographic device based on the detection of fluorescent X-rays, Nuclear Instruments Methods Phys. Res. A277 (1989) 669–672.
[8] H. Neij, B. Johansson, M. Aldén, Development and demonstration of 2D-LIF for studies of mixture preparation in SI engines, Combustion and Flame 99 (1994) 449–457.
[9] J. Lakowicz, Principles of Fluorescence Spectroscopy, Plenum Press, London, Chap. 1, 1983.
[10] J. Miller, Standards in Fluorescence Spectrometry Ultraviolet Spectrometry Group, Chapman & Hall, London, 1981, pp. 5–6.
[11] T. Dreier, A. Dreizler, J. Wolfrum, The application of a Raman-shifted tunable KrF excimer laser for laser-induced fluorescence combustion diagnostics, Appl. Phys. B: Photophys. Laser Chem. B55 (4) (1992) 381–387.
[12] P. Andresen, H. Schluter, D. Wolff, H. Voges, A. Koch, W. Hentschel, W. Oppermann, E. Rothe, Identification and imaging of OH ($v' = 0$) and O/sub 2/($v' = 6$ or 7) in an automobile spark-ignition engine using a tunable KrF excimer laser, Appl. Optics 31 (36) (1992) 7684–7689.
[13] H. Philipp, A. Plimon, A. Fernitz, A. Hirsch, G. Fraidl, E. Winklhofer, A tomographic camera system for diagnostics in SI engines, SAE 950681 (1995).
[14] J.R. Lakowicz, Principles of Fluorescence Spectroscopy, Plenum Press, New York, 1983.
[15] B. Ruck, P. Pavloski, A fast laser-tomography system for flow analyses, in: Int. Conf. Optical Methods Data Processing in Heat and Fluid Flows, IMechE, 1998, p. 465.
[16] K. Kim, M. Choi, C. Lee, W. Kim, In-cylinder fuel distribution measurements using PLIF in an SI engine, SAE 970509 (1997) 83.
[17] D. Hansen, E. Lee, Radiative and nonradiative transitions in the first excited singlet state of symmetrical methyl-substituted acetones, J. Chem. Phys. 62 (1975) 183.
[18] B. Berlman Isadore, Handbook of Fluorescence Spectra of Aromatic Molecules, 2nd Edition, Academic Press, London, 1971.
[19] C. Morgan, A. Mitchell, N. Peacock, J. Murray, High-frequency modulated light source phase fluorometry and fluorescence lifetime imaging, Rev. Sci. Instrum. 66 (1995) 48–51.
[20] S. Nakamura, Light emission moves into the blue, Phys. World 11(2), 1998 and references therein.
[21] A. McGonigle, D. Coutts, C. Webb, A 10 kHz Cerium LiCAF laser pumped by the sum frequency mixed output of a copper vapour laser, in: Conf. Lasers and Electro-Optics Europe, Glasgow, 14–18 September 1998, paper CWJ6.
[22] R. Koch, Th. Schroder, ,U. Stamm W. Zschocke, D. Basting, High Average Power, High Pulse Repetition Frequency Diode Pumped UV Solid-State Laser System, in: Conf. Lasers and Electro-Optics Europe, Glasgow, 14–18 September 1998, paper CWJ5.
[23] R. Conroy, A. Kemp, G. Friel, B. Sinclair, J. Ley, A Comparison of Deflective Q-Switches, in: Conf. Lasers and Electro-Optics Europe, Glasgow, 14–18 September 1998, paper CME8.
[24] Rainbow Photonics AG, Einsteinstrasse, HPF-E7, CH-8093, Zürich. http://www.rainbowphotonics.ethz.ch